Formation and surface-stabilizing contributions to bare nanoemulsions created with negligible surface charge

Andrew P. Carpenter[a], Emma Tran[a], Rebecca M. Altman[a], and Geraldine L. Richmond[a,1]

[a]Department of Chemistry and Biochemistry, University of Oregon, Eugene, OR 97403

Contributed by Geraldine L. Richmond, March 22, 2019 (sent for review January 16, 2019; reviewed by Masafumi Fukuto and Christopher J. Mundy)

The stabilization of nanoemulsions, nanosized oil droplets dispersed in water, is commonly achieved through the addition of surfactants and polymers. However, nanoemulsions in the absence of emulsifiers have been observed to acquire a significant negative charge at their surface, which ultimately contributes to their stability. While the source of this negative charge is disputed to this day, its presence is taken as an inherent property of the aqueous–hydrophobic interface. This report provides a look at the molecular structure and bonding characteristics of bare aqueous–hydrophobic nanoemulsion interfaces. We report the creation of bare nanoemulsions with near zero surface charge, which are marginally stable for several days. The process of creating these low-charge nanoemulsions (LCNEs) required rigorous cleaning procedures and proper solvent storage conditions. Using vibrational sum-frequency scattering spectroscopy, we measure the structure and bonding of the interfacial aqueous and hydrophobic phases. The surfaces of these LCNE samples possess a measurable free OH vibration, not found in previous studies and indicative of a clean interface. Tuning the nanoemulsion charge through addition of anionic surfactants, modeling potential surface-active contaminants, we observe the free OH to disappear and a reorientation of the interfacial hydrophobic molecules at micromolar surfactant concentrations. Notably, the free OH vibration provides evidence for stronger dispersion interactions between water molecules and the hydrophobic phase at the LCNE surface compared with similar planar water–alkane interfaces. We propose the stronger bonding interactions, in addition to an ordered interfacial aqueous layer, contribute to the delayed droplet coalescence and subsequent phase separation.

nanoemulsions | surface spectroscopy | interfacial water | vibrational sum-frequency scattering spectroscopy | oil–water interfaces

There has been a growing interest in emulsion particles in the nanoscale regime due to their unique potential for applications in drug delivery (1), in oil recovery (2), and as nanoreactors for producing a range of nanomaterials including polymers and semiconductor quantum dots (3, 4). Relative to micelles, little is known about the interfacial molecular processes leading to the formation and stability of such nanoemulsions. Key to advancing the utility of these and related nanoscale liposome systems is much-needed molecular-level characterization of the structure and bonding interactions at the surface of these soft nanoparticles.

Although most nanoemulsions are stabilized by various surfactant systems, recent studies report nanoemulsions stabilized without added surfactants (5–8). Such reports beg the question as to what interfacial molecular factors are responsible for such stabilization. Electrophoretic mobility (EpM) measurements of these nanoemulsions show they possess a negative surface charge that is attributed to surface enhancement of hydroxide ions that act as a primary stabilizing factor. Other studies of bare negatively charged nanoemulsions including surface vibrational sum-frequency scattering spectroscopy (VSFSS) measurements have invoked other droplet stabilizing factors including electric fields established by ordered water dipoles, charge transfer models from asymmetric hydrogen bonding environments, and the presence of trace amounts of surface-active adsorbates (9–12).

Herein, we report the creation of nanoemulsions with nearly zero surface charge. These hexadecane/water nanoemulsions have a droplet size of ∼300 nm that persists over several days. EpM and VSFSS studies of these low-charge nanoemulsions (LCNEs) show that interfacial water and oil have very different molecular bonding and orientation than found for the more negatively charged surfactant-free nanoemulsions (9, 10, 13). For example, the surface of our LCNEs contain a free OH vibration, measured by VSFSS, which was not found in the previous spectroscopic studies (10). The frequency of this free OH indicates there is a stronger water bonding interaction with the hexadecane, compared with the planar interface, a factor we conclude contributes to droplet stabilization. These results are important for understanding water–hydrophobic interactions in general, and notably for hydrophobic droplets in the nanosized regime.

Nanoemulsion Surface Spectroscopy

VSFSS (Fig. 1) was used here to investigate the surface structure and bonding of the aqueous and hydrophobic phases in LCNE dispersions. Pioneered and developed by the Roke group (14), VSFSS measures the vibrational spectrum of interfacially adsorbed and ordered molecules without contribution from bulk molecules (15, 16). Through polarization selection of the incident and detected beams, specific net dipole moment orientations can be detected (17). Spectra reported here, for both phases, are recorded in the PPP and SSP polarization combinations, where the letters correspond to the polarization of the sum-frequency, visible, and IR beams, respectively. The SSP polarization combination samples

Significance

There is a growing view that the bare water–hydrophobic interface spontaneously acquires a significant negative charge. Recent bare nanoemulsion studies support this notion, invoking the charge as the primary stabilizing factor. This study reports the creation of bare nanoemulsions that have moderate stability but nearly zero negative surface charge. Surface spectroscopic studies show that there is an enhanced bonding between oil and water at the droplet surface relative to a comparable planar interface that is concluded to be a contributing factor to their stabilization. The results are relevant to soft water–hydrophobic interfaces in the presence and absence of charge that are common in nanosized biological, geological, and environmental systems.

Author contributions: A.P.C. and G.L.R. designed research; A.P.C., E.T., and R.M.A. performed research; A.P.C. analyzed data; and A.P.C. and G.L.R. wrote the paper.

Reviewers: M.F., Brookhaven National Laboratory; and C.J.M., Pacific Northwest National Laboratory.

The authors declare no conflict of interest.

Published under the PNAS license.

Data deposition: All data appearing in this work are available from the corresponding author upon reasonable request.

[1]To whom correspondence should be addressed. Email: richmond@uoregon.edu.

This article contains supporting information online at www.pnas.org/lookup/suppl/doi:10.1073/pnas.1900802116/-/DCSupplemental.

Published online April 24, 2019.

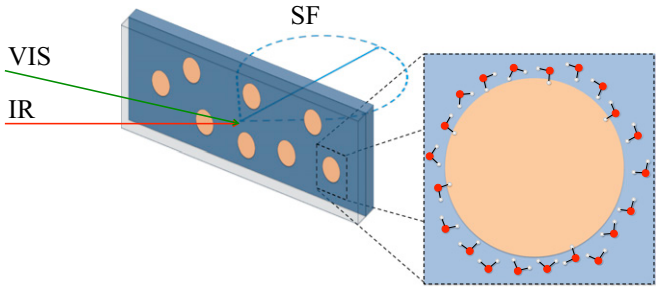

Fig. 1. Surface spectroscopy of bare nanoemulsions. Illustration of VSFSS experimental geometry probing oil droplets dispersed in water inside a quartz experimental cuvette with a CaF_2 front window (back and front panels, respectively). A femtosecond IR beam is overlapped with a picosecond visible beam, generating a sum-frequency response off the droplet surface. (*Inset*) The droplet is a representation of the bare nanoemulsion and the first layer of water molecules.

surface molecular dipole components perpendicular to the droplet surface (14, 17, 18). Related vibrational sum-frequency spectroscopy (VSFS) experiments, conducted herein, at planar interfaces aid in the assignment of droplet spectral features and in understanding molecular factors contributing to nanoemulsion stabilization.

The VSFSS and VSFS experimental systems used in these studies have been previously reported (18, 19). In brief, a femtosecond broadband laser system was used for the droplet VSFSS experiments, while a picosecond laser system was used for the planar VSFS experiments (*SI Appendix*). For the droplet experiments, both the high-energy deuterated water stretching region (2,600–2,800 cm^{-1}) and the CH stretching region (2,800–3,000 cm^{-1}) were measured to understand the structure and composition of the interfacial water and oil molecules, respectively. In the aqueous-phase VSFSS experiments, the IR beam passes through the bulk aqueous phase and is absorbed by the D_2O molecules. Therefore, these experiments were performed using a 50:50 mixture of D_2O:H_2O, hereafter referred to as HOD, to reduce the IR absorption by D_2O molecules in the continuous aqueous phase. HOD molecules are made by mixing H_2O and D_2O, with the equilibrium HOD and D_2O concentrations in our experiments constituting 50% and 25% of the aqueous phase, respectively. The reduced amount of D_2O molecules leads to a higher transmission of the IR beam, leading to successful excitation of water at nanoemulsion surfaces in these studies. To understand the aqueous-phase droplet spectroscopy experiments in further detail, both HOD and D_2O were studied at the aqueous–CCl_4 interface as a model aqueous–hydrophobic system, similar to previous work out of this laboratory (20).

LCNEs

The bare nanoemulsions in this study were made by sonicating hexadecane [1% (vol/vol)] into a neat aqueous solution, resulting in a droplet size of ∼300 nm (measured by dynamic light scattering). Hexadecane was chosen to be consistent with the majority of literature. Droplet coalescence and phase separation were not observed to occur as quickly as expected. It was found the nanoemulsion suspensions would cream out daily as the droplets rose to the top of the solution due to buoyant forces. However, when the solution was redispersed by shaking, and particle size remeasured, changes to the droplet size were negligible. Over a week's time, the nanoemulsion solution becomes increasingly translucent, indicative of a lower droplet volume fraction. Coincident with these observations is the appearance of a thin oil layer on top of the aqueous layer. As a result of the higher droplet density at the top of the solution after the nanoemulsions have creamed out, the rate of coalescence will increase in this region, explaining the decrease in droplet volume fraction over the course of a week.

Zeta potential (ZP) values for bare nanoemulsion solutions were measured with a Zetasizer ZS (Malvern), using the Huckel relationship to calculate the ZP from EpM values. While more advanced relationships have been developed (21), the Huckel relationship is appropriate for nanoemulsion dispersions in low ionic strength solutions, such as the samples in this study. The nanodroplets examined here were prepared in pH 7 solutions and possessed ZP values of −9.7 ± 5 mV (Fig. 2, green stripe). Previous studies of hexadecane bare nanoemulsions have measured ZP values between −55 and −80 mV when suspended in pH-neutral solutions (Fig. 2, black stripe) (5–10). Clearly, the bare nanoemulsions prepared in this work possess ZP values much smaller than previously reported values. This is true for the EpM values from which these ZP values are calculated. The low ZP for these bare nanoemulsions is a direct result of a stringent multistep cleaning procedure to avoid any potential surface contaminants (*SI Appendix*). Fig. 2 demonstrates the sensitivity of the measured ZP to the glassware cleaning procedure (red stripe) and aqueous solvent storage conditions (purple stripe). These trends are consistent for nanoemulsions created with HOD, H_2O, and D_2O aqueous phases. While we would be naive to conclude our bare nanoemulsion surfaces are immaculate, it is clear from our EpM and VSFSS experiments discussed below that contaminants have been minimized to a new level.

As a result of these observations, all LCNE samples were prepared with aqueous and hydrophobic phases consisting of ultrapure H_2O (18.2 MΩ·cm resistivity) and high-purity hexadecane (≥99%), respectively. All glassware was cleaned in a two-stage acid bath cleaning procedure (*SI Appendix*). The preparation procedures used here mirror what we have routinely used in our planar oil–water studies since we demonstrated the remarkable VSF sensitivity in the water OH stretching region to nanomolar levels of contaminants (22).

Water Bonding and Hydrophobic Structuring at the LCNE Surface

The characteristic signature of a bare oil–water interface we have sought to measure is that of water molecules straddling the interface with one bond oriented into the oil-rich phase [referred to as the free OH(OD)]. The vibrational frequency of the energetically uncoupled free OH (OD) mode is found to be sensitive to dispersion interactions with the oil phase, resulting in a shift to lower frequencies upon stronger intermolecular interactions (20, 23). This mode is diminished and often absent in the presence of surfactants or contaminants, usually concomitant with an enhancement of the VSF signal at lower frequencies corresponding to

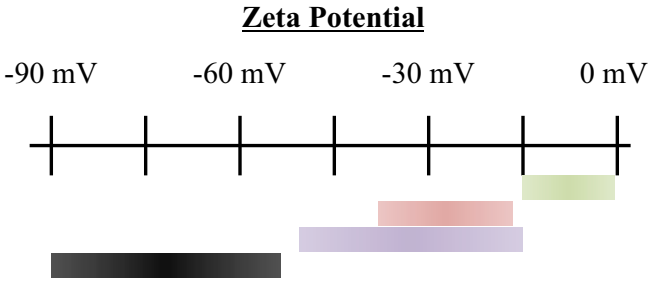

Fig. 2. ZP values from different sources. Representation of the ZP value ranges of bare nanoemulsion samples. The ZP value ranges for samples from this work, prepared in glassware cleaned in isolated acid baths (green), in "contaminated" acid baths (red), and with aqueous phases stored in low-quality polyethylene (purple), are compared with a range of values commonly found in literature (black).

strongly coupled interfacial water molecules (22). VSFS has previously been our method of choice for understanding the structure and bonding environment of the interfacial water region at the planar oil–water interface (20) and is used here to provide a comparison with how the interfacial structuring changes with the curvature of the interface (14, 18).

VSFSS experiments of the aqueous phase, in both PPP and SSP polarization, reveal a vibrational resonance near 2,700 cm^{-1} (Fig. 3, *Inset*). After normalizing to the HOD IR transmittance and broadband IR pulse profile (*SI Appendix*), this resonance appears as a shoulder on top of a broader lower energy resonance (Fig. 3). This peak is assigned to the free OD modes of HOD and D_2O molecules straddling the droplet surface. This is consistent with the low-intensity free OH previously observed at planar alkane–water interfaces (23, 24). A search for possible artifacts, such as HOD at the CaF_2 cuvette window, did not reveal any similar resonance seen in the VSFSS experiments. Additionally, the free OD found in these experiments disappears in the presence of surfactants, discussed below, consistent with previous planar oil–water studies (25). Thus, as its behavior matches that of a free OD resonance, we assign it as such.

As noted above, the free OD frequency is sensitive to the water–oil bonding interactions (20). The experimentally simpler planar studies of HOD–CCl_4 and D_2O–CCl_4 interfaces were performed to assist in understanding contributing spectral features at the droplet surface (*SI Appendix*). These studies reveal there exist two free OD oscillators from HOD and D_2O contributing to the free OD signal in Fig. 3, consistent with what has been observed for the air–water interface (26). A previously described fitting routine (18, 24, 27) was used to determine the frequency of the droplet free OD for the PPP spectrum, as the signal intensity is greater than for SSP (*SI Appendix*). The results of this fitting routine place the droplet HOD free OD oscillator at 2,688 ± 2 cm^{-1}, a red shift of ∼17 cm^{-1} relative to what is expected for a planar HOD–hexadecane interface (2,705 cm^{-1}; *SI Appendix*). A red shift of this magnitude is indicative of stronger water–oil dispersion bonding interactions at the droplet interface relative to the similar planar water–alkane interface (20). While the full coordinated water spectrum cannot be measured for these oil droplet surfaces due to strong IR absorbance at lower wavenumbers, it can be concluded specific contributions from weakly hydrogen bonded species contribute to the rise in intensity at frequencies below 2,680 cm^{-1} (23).

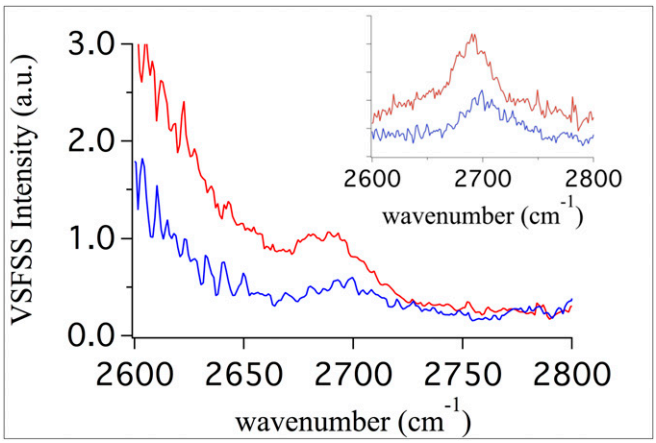

Fig. 3. Free OD resonance at the LCNE droplet surface. Spectra of the high-energy portion of the D_2O stretching region recorded in the PPP (red) and SSP (blue) polarization combinations. After normalization by both the IR pulse profile and the IR transmission spectrum of the HOD continuous phase, the free OD appears as a shoulder on top of a broader resonance in the fully normalized spectra. *Inset* shows the spectra prenormalization.

To investigate the interfacial hexadecane ordering, VSFSS studies of our LCNE surfaces were performed in the CH stretching region using both SSP and PPP polarization combinations (Fig. 4 and *SI Appendix*, Fig. S6, respectively). The VSF scattering signal from the CH modes of hexadecane was found to be very weak for both sets of polarization conditions and barely discernable from the background noise in the SSP experiments. The CH stretching vibrations would be minimally sum-frequency active in the SSP polarization combination for hexadecane molecules oriented parallel to the droplet surface. Thus, the nearly flat spectral response found in the SSP spectra, and minimal response in PPP polarization combination, indicate the interfacial hexadecane lies relatively parallel to the interface. This is consistent with X-ray reflectivity measurements and molecular dynamics simulations (28). Furthermore, the presence of a minimal CH stretching response for bare hexadecane droplets supports computational work concluding there must exist a rough alkane surface necessary to provide space for a free OD to exist (12). If the hydrophobic phase was atomically flat, the hydrophobic pockets required for a free OD would not exist, resulting in no free OD resonance and no SF active CH stretching modes. Additionally, we find the CH stretching response is greatly enhanced upon addition of deuterated anionic surfactants as discussed below.

Our results differ from previous VSFSS experiments seeking to measure interfacial water and hexadecane contributions. Since the free OD resonance was not detectable in the previous studies, it was concluded that the free OD is absent at bare nanoemulsion surfaces (10). However, those VSFSS experiments were complicated by IR absorbance of the continuous D_2O phase and also were performed on nanoemulsions with ZP values of −55 mV, nearly an order of magnitude greater than those reported here. As discussed later, we conclude this higher charge is a potential contributor to the absence of a free OD at nanoemulsion surfaces. Another VSFSS study of reverse nanoemulsions stabilized by 5 mM Span 80 was able to access much more of the OD stretching region of the interfacial water (29). No free OD mode was observed in those spectra either. These Span 80-coated nanoemulsions did, however, have a larger signal from coordinated water compared with the Span 80-covered planar air–water interface. From this, it was concluded water at the droplet surface has stronger interfacial water bonding. However, our measurements performed directly on a Span 80-covered planar oil–water interface show enhanced water bonding that is very similar to what is found in the previous studies of Span 80-coated nanodroplets (*SI Appendix*). Our contrary results draw into question whether there is an enhanced water hydrogen-bonding network that is a contributing factor in nanoemulsion stabilization.

On the hexadecane side, previous VSFSS studies of these highly negatively charged nanoemulsions obtained a strong spectral response from the CH modes of the surface hexadecane molecules (9, 13). It was concluded the presence of some anionic surfactants failed to perturb the hydrophobic phase, and both the surfactant and hexadecane molecules oriented themselves parallel to the droplet surface. As noted in more detail below, for our LCNE nanoemulsions, the addition of surfactant greatly enhances the otherwise-low VSFS signal of hexadecane CH modes.

Investigating and Tuning the Droplet Charge

To reconcile the differences in spectral measurements conducted with our LCNE droplets and those nanodroplets possessing much higher ZPs, we performed studies where the droplet charge was progressively increased by adsorption of anionic surfactants. The added surfactant is not assumed to have identical molecular characteristics of any surface adsorbed species or impurity that might have been present in previous nanodroplet studies with more negative ZPs. They are merely used as a mechanism for

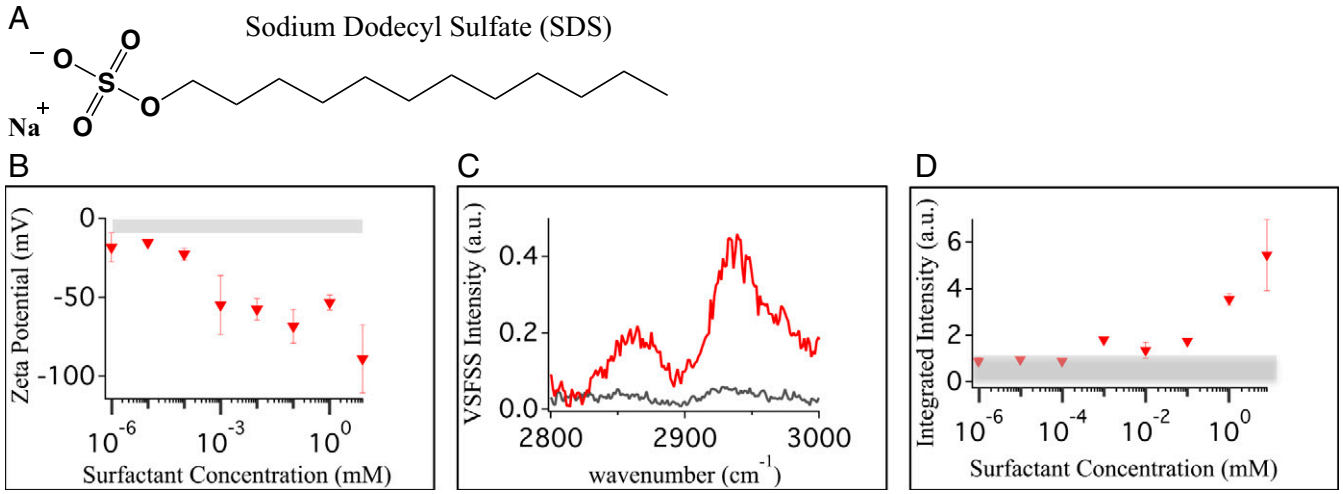

Fig. 4. Tuning droplet charge with surfactant addition. The surfactant SDS (*A*) was used to tune the nanoemulsion charge. The ZP (*B*) is plotted as a function of SDS concentration, with the gray bar highlighting the ZP for LCNE samples in this study. (*C*) SSP spectra of the CH stretching region (2,800–3,000 cm^{-1}) of bare LCNE (gray) and deuterated SDS stabilized (1 mM) nanoemulsions. (*D*) SSP signal from interfacial hexadecane in the CH stretching region was integrated for deuterated SDS (red) stabilized nanoemulsions. The gray box brackets the integrated response for bare nanoemulsions taken on the same days as the surfactant-stabilized nanoemulsions.

charging the interface. Our studies examined the sensitivity of the nanoemulsion ZP, free OD, and ordering of the hydrophobic phase to the presence of surface adsorbants. Nanoemulsions were created with the deuterated anionic surfactant SDS (Fig. 4*A*) dissolved in the aqueous phase. All surfactant-stabilized nanoemulsion samples had average diameters around 300 nm, similar to the bare nanoemulsions. EpM measurements of these samples mark a clear decrease (more negative) in ZP as the bulk surfactant concentration increases (Fig. 4*B*). It is observed that nanomolar surfactant concentrations decrease the ZP value from that of bare nanoemulsions.

To determine the surfactant concentration where the droplet free OD disappears, VSFSS experiments were performed on nanoemulsions with high surfactant concentrations (1 μM to 1 mM). Consequentially, we observe the free OD to disappear when surfactant concentrations exceed 10 μM. At higher surfactant concentrations, the free OD oscillator intensity is reduced by an exclusion of the available surface area for free OD oscillators at the droplet surface. Additionally, bonding interactions between the surfactant and free OD water molecules will result in a redshift of the vibrational mode out of the spectral window. The full procedure used to determine our estimate is included in *SI Appendix*. Briefly, a LCNE sample was first measured to ensure proper experimental setup. Following identification of the free OD from a LCNE sample, a series of nanoemulsion samples with decreasing amounts of surfactant were measured until a free OD resonance was seen. Nanoemulsions prepared with a 10 μM surfactant concentration were seen to possess a free OD, while nanoemulsion samples in 100 μM surfactant concentration did not. The corresponding ZP for droplets with 10 μM SDS is near −50 mV, near ZP values common in literature.

To investigate the effect surfactants have on the interfacial structure of the LCNE hydrophobic phase, the interfacial hexadecane CH stretching modes were measured with VSFSS upon addition of deuterated SDS to the aqueous solution. To resolve the vibrational spectrum of the hexadecane alkyl chains, deuterated surfactants were used to remove spectral interferences from surfactant alkyl chains. As noted above, and shown in Fig. 4 *C* and *D*, the CH spectral response from surfactant-free LCNE samples measured in SSP and PPP polarization combinations is low. Using the SSP and PPP polarization combinations, any CH signal observed originates from ordered hexadecane alkane chains at the droplet surface. A dramatic change occurs, however, upon addition of 1 mM deuterated SDS (Fig. 4*C* and *SI Appendix*, Fig. S6). Surfactant addition results in a significant increase in CH spectral response from hexadecane methylene and methyl CH stretch modes in both SSP and PPP polarizations. Clearly, the added surfactant causes a strong net reorientation of the hexadecane chains.

Further VSFSS studies of surfactant-induced reorientation of interfacial hexadecane were conducted for nanoemulsions stabilized with surfactant concentrations spanning 1 nM to 8 mM. Spectra were normalized by the calculated scattering intensity at 60° of each sample to account for droplet size-dependent changes to the measured signal intensity. Integrating the SSP spectral response across the CH stretching region (2,800–3,000 cm^{-1}), it is clear there is a progressive increase in signal intensity from the interfacial hexadecane as the deuterated surfactant concentration increases (Fig. 4*D*). The intensity increase is a result of a reordering of the interfacial hexadecane. Similar to the free OD behavior, this effect becomes noticeable with surfactant concentrations of 10 μM and ZP values near −50 mV, near the ZP values common in the literature for bare nanoemulsion samples (7, 8, 10, 13, 25). We also observed these behaviors for nanoemulsions prepared with deuterated potassium laurate, a carboxylic acid-based surfactant (*SI Appendix*). The increase in integrated VSFSS signal here follows the same trend as seen for added SDS. For potassium laurate-stabilized nanoemulsions, the free OD also disappears when the surfactant concentration exceeds 10 μM.

This restructuring of the interfacial hexadecane molecules is a direct result of surfactant molecules reorienting portions of the hydrophobic phase. After a critical concentration of surfactant molecules populating the interface, the surfactant alkyl chains perturb the interfacial hexadecane molecules. Our SSP polarization VSFSS experiments suggest this reorientation manifests itself as more hexadecane alkyl chains aligning perpendicular to the droplet surface. Previous molecular dynamics simulations from our laboratory, in addition to second harmonic and sum frequency scattering experiments of others, have demonstrated surfactant headgroup solvation helps align the first few carbons in the surfactant alkyl chain at the oil–water interface (30, 31). As the surfactants in our experiments populate the interface, the first few carbons in the surfactant chain will be ordered in a way that encourages interfacial hexadecane to reorient portions of the alkyl chain to maximize chain–chain interactions.

The importance of chain–chain interactions between the stabilizing surfactant and the interfacial hydrophobic phase cannot be understated. Several groups have found the oil droplet shape is spontaneously altered by slow temperature variation (32–35). While the mechanism of these morphological transitions is currently under debate, experiments reveal the transition is affected by the length of the surfactant relative to the oil phase and is invariant of the headgroup charge (anionic, cationic, nonionic) (34), implying the intermolecular interactions between the surfactants and hydrophobic phase play an important role (34). Ongoing experiments in this laboratory seek to understand why these chain–chain interactions are so important.

LCNE Stabilization Mechanism

The LCNE nanoemulsions reported herein clearly have surface properties that are distinct from those previously reported with higher surface charges. We attribute our ability to produce these unique nanodroplets to preparation procedures that minimize the contaminants we found when producing nanoemulsions with ZPs more negative than −55 mV. If not a negative charge, what then is contributing to LCNE stabilization? As the droplets are dispersed in solution, after sonication, the droplet volume is low [1% (vol/vol)], making droplet coalescence a rare event. Within 24 h, the majority of LCNE droplets are observed to cream to the top of the aqueous dispersion. The droplet density at the top of these solutions is greatly increased relative to the initial dispersed condition, and during this stage of higher volume fractions, droplet coalescence is more likely. As two droplets approach one another, the aqueous thin film between the two droplets must drain for coalescence to occur.

Clearly, our spectroscopy experiments of the aqueous phase indicate the water–oil bonding interactions are greater at the droplet surface and thus provide a greater stability of the interdroplet aqueous film relative to the planar interface. We believe the stronger dispersion interactions are playing a role in the droplet stabilization. It has been observed for bubbles that if the interdroplet thin film drainage time is long, relative to the collision time of two droplets, coalescence and subsequent phase separation will be delayed (36). We speculate the stronger water–oil bonding interactions at the LCNE droplet surface may result in a reduced flow rate of the interdroplet aqueous film, resulting in a lower drainage time and thus lower collision frequency, leading to greater droplet stability. Additionally, coincident with the free OD will be an extended hydrogen-bonding network (23). It is possible this hydrogen-bonding network is also contributing to the droplet stability as a slight interfacial field has been calculated from the ordered surface dipole of highly oriented surface water molecules (12, 37, 38). This field would assist in the stabilization by providing a slight electrostatic repulsion between droplet surfaces. The significance of contributions such as the affect interfacial water structure has on droplet stability requires more experiments and computational modeling.

With regards to contributing factors previously invoked to explain the nanoemulsions stabilization of those with ZP measurements in the range of between −50 and −80 mV, most assume the surface charge is a contributing factor in some form or another (5–10). In the case of the hydroxide ion as a contributing factor, it is possible there are small amounts of hydroxide ions at the LCNE interface that could be contributing to the small ZPs measured. However, there is no spectral evidence for a surface excess of hydroxide ions in our aqueous phase spectra or in previous work by Samson et al. (10) Previous computational work concluded that any surface excess of hydroxide would be oriented at the droplet surface as a result of the interfacial electric fields (12, 37, 38). Given estimates of a surface area/hydroxide of 3 nm^2 (8), one would expect a vibrational resonance for adsorbed deuterated hydroxide ($^{-}$OD) ions to appear in our spectrum near 2,725 cm^{-1} (Fig. 2) (10), of which we find no evidence. Vácha et al. concluded droplet stabilization is due to an interfacial charge resulting from a charge transfer process within the asymmetric hydrogen-bonding environment at the droplet interface (9). With the low charges of our LCNEs, such a charge transfer model is unnecessary. Our surfactant addition studies, which create nanoemulsions with more negative ZPs, are able to reproduce the observations of previous VSFSS studies of presumed bare nanoemulsions. The results of our studies suggest surface adsorbates are responsible for the significant negative charge, which is in agreement with previous studies suggesting adsorbates are a factor in the formation of negatively charged and presumed bare nanoemulsions (11, 39–41).

Summary

The bare nanoemulsion surface is a model for systems possessing nanosized aqueous–hydrophobic interfaces. This work is focused on bare nanoemulsions prepared without the significant negative surface charge that is routinely reported by others to be a stabilizing factor. This report provides important insights into the interfacial bonding and structure at the aqueous–hydrophobic droplet interface where contaminants or other added surfactants have been minimized. Instead of relying on indirect phase interference arguments and surfactant-coated water droplets (9, 10, 29), this study provides direct measurements of the interfacial aqueous layer in contact with the bare nanoemulsion surface. Success in preparing and characterizing the bonding interactions at these bare droplet surfaces have also provided a more accurate understanding of how interfacial bonding and solvent orientation are altered by the presence of surfactants.

EpM measurements, used to measure the surface charge at these LCNE droplet surfaces, demonstrate how the presence of nanomolar surface impurities increase the surface charge. These experiments support the notion the large negative charge previously observed to accumulate at hydrophobic droplet surfaces is likely the result of surface-active impurities. The idea of surface impurities giving rise to larger ZP values is not new. Work with surfactant stabilized nanoemulsions, as well as recent work

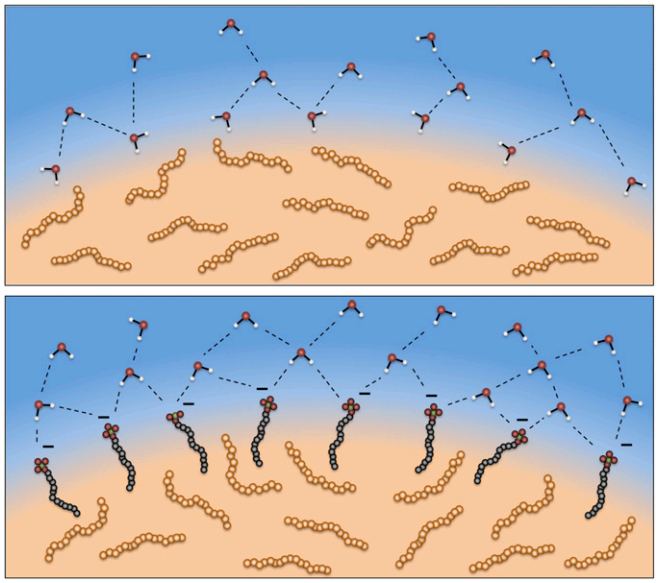

Fig. 5. Bare and surfactant covered surfaces. Illustration of the nanoemulsion surfaces for bare (*Top*) and surfactant-covered (*Bottom*) nanoemulsions. Hexadecane molecules lie relatively parallel to the bare droplet surface, providing room for free OD oscillators. When surfactants cover the droplet surface, a reorientation of the hexadecane occurs due to chain–chain interactions and the free OD is excluded.

investigating the origins of the Jones–Ray effect, have demonstrated nanomolar concentrations of surfactant impurities can have significant effects on macroscopic observables, that is, surface tension and EpM measurements (11, 39–41). The surface spectroscopic technique VSFSS, applied here, has provided a direct means of isolating and investigating the presence and effects of any surface impurities on the droplet surface structure.

Our success in spectroscopically measuring the free OD and hexadecane at the LCNE droplet surface provides insight into the water–hexadecane bonding interactions at the nanodroplet surface that were not accessible in previously studies. Water at the LCNE droplet surface is found to participate in stronger dispersion bonding interactions with the interfacial oil molecules compared with the planar oil–water interface. The presence of the free OD and spectral features of the CH stretching modes of interfacial hexadecane form a roughened surface where the alkane molecules are largely oriented flat relative the LCNE surface. We conclude the bonding characteristics of water with the oil phase are a contributing factor to LCNE stability with ongoing experiments in this laboratory focused on exploring in detail of how structural changes of the interfacial aqueous and hydrophobic phases alter LCNE droplet stability.

When surfactants were added to tune the interfacial charge, the ZP became more negative, concomitant with spectral characteristics similar to those seen in previous VSFSS studies. The free OD was seen to disappear at higher surfactant concentrations, consistent with the behavior of the free OH at planar aqueous–hydrophobic interfaces (20, 23, 24). Additionally, as surfactant concentrations increase, the surface ordering of interfacial hexadecane molecules was seen to increase. This reordering of the hydrophobic phase, illustrated in Fig. 5, was not observed in previous VSFSS experiments. However, those nanoemulsions possessed much more negative ZPs, likely from surface adsorbants. From our experiments, it is clear surface-adsorbed surfactants perturb the aqueous and hydrophobic phases at concentrations undetectable by surface-specific spectroscopies. Our work here provides the clearest view of bare nanoemulsion surfaces and changes to the molecular structure resulting from surface adsorbants. Ongoing work in this laboratory is focused on using LCNE samples to understand the structure and bonding characteristics of nanosized aqueous–hydrophobic surfaces. With current interest in the structure and bonding present at the aqueous–hydrophobic interface, this report provides crucial details of the bare nanoemulsion interface that are important to the proper study and modeling of nanosized aqueous–hydrophobic interfaces.

ACKNOWLEDGMENTS. We thank Larry Scatena for particularly insightful discussions regarding interfacial water. This material is based upon work supported by the US Department of Energy, Office of Science, Condensed Phase and Interfacial Molecular Science Division under Award DE-SC0014278.

1. Szczepanowicz K, et al. (2015) Biocompatible long-sustained release oil-core polyelectrolyte nanocarriers: From controlling physical state and stability to biological impact. *Adv Colloid Interface Sci* 222:678–691.
2. Czarnecki J (2009) Stabilization of water in crude oil emulsions. Part 2. *Energy Fuels* 23:1253–1257.
3. Eastoe J, Hollamby MJ, Hudson L (2006) Recent advances in nanoparticle synthesis with reversed micelles. *Adv Colloid Interface Sci* 128-130:5–15.
4. Muñoz-Espí R, Álvarez-Bermúdez O (2018) Application of nanoemulsions in the synthesis of nanoparticles. *Nanoemulsions: Formulation, Applications, and Characterization*, eds Jafari SM, McClements DJ (Academic, London), pp 477–515.
5. Beattie JK (2007) The intrinsic charge at the hydrophobe/water interface. *Colloid Stability: The Role of Surface Forces—Part II*, ed Tadros TF (Wiley-VCH, Weinheim, Germany), Vol 2, pp 153–164.
6. Beattie JK, Djerdjev AM, Warr GG (2009) The surface of neat water is basic. *Faraday Discuss* 141:31–39; discussion 81–98.
7. Djerdjev AM, Beattie JK, Hunter RJ (2003) Stagnant layer conduction in surfactant-stabilized hexadecane emulsion systems measured by electroacoustics. *Aust J Chem* 56:1081–1089.
8. Creux P, Lachaise J, Graciaa A, Beattie JK, Djerdjev AM (2009) Strong specific hydroxide ion binding at the pristine oil/water and air/water interfaces. *J Phys Chem B* 113:14146–14150.
9. Vácha R, et al. (2011) The orientation and charge of water at the hydrophobic oil droplet-water interface. *J Am Chem Soc* 133:10204–10210.
10. Samson J-S, Scheu R, Smolentsev N, Rick SW, Roke S (2014) Sum frequency spectroscopy of the hydrophobic nanodroplet/water interface: Absence of hydroxyl ion and dangling OH bond signatures. *Chem Phys Lett* 615:124–131.
11. Roger K, Cabane B (2012) Why are hydrophobic/water interfaces negatively charged? *Angew Chem Int Ed Engl* 51:5625–5628.
12. Knecht V, Risselada HJ, Mark AE, Marrink SJ (2008) Electrophoretic mobility does not always reflect the charge on an oil droplet. *J Colloid Interface Sci* 318:477–486.
13. Scheu R, et al. (2014) Specific ion effects in amphiphile hydration and interface stabilization. *J Am Chem Soc* 136:2040–2047.
14. Roke S, Gonella G (2012) Nonlinear light scattering and spectroscopy of particles and droplets in liquids. *Annu Rev Phys Chem* 63:353–378.
15. Roke S, et al. (2003) Vibrational sum frequency scattering from a submicron suspension. *Phys Rev Lett* 91:258302.
16. Roke S, Bonn M, Petukhov AV (2004) Nonlinear optical scattering: The concept of effective susceptibility. *Phys Rev B* 70:115106.
17. de Beer AGF, Roke S (2010) Obtaining molecular orientation from second harmonic and sum frequency scattering experiments in water: Angular distribution and polarization dependence. *J Chem Phys* 132:234702.
18. Hensel JK, et al. (2017) Molecular characterization of water and surfactant AOT at nanoemulsion surfaces. *Proc Natl Acad Sci USA* 114:13351–13356.
19. Schabes BK, Altman RM, Richmond GL (2018) Come together: Molecular details into the synergistic effects of polymer-surfactant adsorption at the oil/water interface. *J Phys Chem B* 122:8582–8590.
20. Moore FG, Richmond GL (2008) Integration or segregation: How do molecules behave at oil/water interfaces? *Acc Chem Res* 41:739–748.
21. O'Brien RW, Hunter RJ (1981) The electrophoretic mobility of large colloidal particles. *Can J Chem* 59:1878–1887.
22. Scatena LF, Richmond GL (2004) Isolated molecular ion solvation at an oil/water interface investigated by vibrational sum-frequency spectroscopy. *J Phys Chem B* 108: 12518–12528.
23. Scatena LF, Brown MG, Richmond GL (2001) Water at hydrophobic surfaces: Weak hydrogen bonding and strong orientation effects. *Science* 292:908–912.
24. Brown MG, Walker DS, Raymond EA, Richmond GL (2003) Vibrational sum-frequency spectroscopy of alkane/water interfaces: Experiment and theoretical simulation. *J Phys Chem B* 107:237–244.
25. Beattie JK, et al. (2014) pH and the surface tension of water. *J Colloid Interface Sci* 422:54–57.
26. Stiopkin IV, et al. (2011) Hydrogen bonding at the water surface revealed by isotopic dilution spectroscopy. *Nature* 474:192–195.
27. Bain CD, Davies PB, Ong TH, Ward RN, Brown MA (1991) Quantitative analysis of monolayer composition by sum-frequency vibrational spectroscopy. *Langmuir* 7: 1563–1566.
28. Fukuto M, et al. (2016) Nanoscale structure of the oil-water interface. *Phys Rev Lett* 117:256102.
29. Smolentsev N, Smit WJ, Bakker HJ, Roke S (2017) The interfacial structure of water droplets in a hydrophobic liquid. *Nat Commun* 8:15548.
30. Holte LK, Kuran BA, Richmond GL, Johnson KE (2014) Computational modeling of lauric acid at the organic–water interface. *J Phys Chem C* 118:10024–10032.
31. Kovacik F, Okur HI, Smolentsev N, Scheu R, Roke S (2018) Hydration mediated interfacial transitions on mixed hydrophobic/hydrophilic nanodroplet interfaces. *J Chem Phys* 149:234704.
32. Guttman S, Ocko BM, Deutsch M, Sloutskin E (2016) From faceted vesicles to liquid icoshedra: Where topology and crystallography meet. *Curr Opin Colloid Interface Sci* 22:35–40.
33. Guttman S, et al. (2016) How faceted liquid droplets grow tails. *Proc Natl Acad Sci USA* 113:493–496.
34. Denkov N, Tcholakova S, Lesov I, Cholakova D, Smoukov SK (2015) Self-shaping of oil droplets via the formation of intermediate rotator phases upon cooling. *Nature* 528: 392–395.
35. Cholakova D, Denkov N, Tcholakova S, Lesov I, Smoukov SK (2016) Control of drop shape transformations in cooled emulsions. *Adv Colloid Interface Sci* 235:90–107.
36. Vakarelski IU, et al. (2010) Dynamic interactions between microbubbles in water. *Proc Natl Acad Sci USA* 107:11177–11182.
37. Hore DK, Walker DS, Mackinnon L, Richmond GL (2007) Molecular structure of the chloroform-water and dichloromethane-water interface. *J Phys Chem C* 111: 8832–8842.
38. Chang T-M, Dang LX (1996) Molecular dynamics simulations of CCl_4-H_2O liquid-liquid interface with polarizable potential models. *J Chem Phys* 104:6772–6783.
39. Duignan TT, et al. (2018) Detecting the undetectable: The role of trace surfactant in the Jones-Ray effect. *J Chem Phys* 149:194702.
40. Takahashi M (2005) ζ potential of microbubbles in aqueous solutions: Electrical properties of the gas-water interface. *J Phys Chem B* 109:21858–21864.
41. Uematsu Y, Bonthuis DJ, Netz RR (2018) Charged surface-active impurities at nanomolar concentration induce jones-ray effect. *J Phys Chem Lett* 9:189–193.